Appendix to the paper "From Earthquake Centroid to Spatial-Temporal Rupture Evolution: Mw 6.3 Movri Mountain Earthquake, June 8, 2008, Greece" by F. Gallovič, J. Zahradník, D. Křížová, V. Plicka, E. Sokos, A. Serpetsidaki, and G-A. Tselentis

Derivation of analytical formula for the misfit derivative

For simplicity we assume a line fault. The j-th component of synthetic seismogram $u_j(\boldsymbol{x}_i, t)$ at receiver $\boldsymbol{x}_i$ can be expressed using the representation theorem (Aki and Richards, 2002),

$$u_j(\boldsymbol{x}_i, t) = W \int_0^T \int_0^L H(\boldsymbol{x}_i; \xi, t-\tau) s(\xi, \tau) d\xi d\tau \tag{1}$$

where $s(\xi, t)$ describes the slip velocity evolution with time t and along the fault position ξ. The fault length and width are denoted L and W, respectively. $H(\boldsymbol{x}_i; \xi, t)$ is the impulse response due to a double couple source located at the fault in a generally inhomogeneous medium evaluated for the given receiver at $\boldsymbol{x}_i$. We seek slip velocity $s(\xi, t)$ without any parameterizations of its spatial-temporal distribution (e.g., by imposing a shape of the slip function, rise time, rupture time, etc.), thus the name "non-parametric inversion".

We define misfit as an L2 norm between synthetic, $u_j(\boldsymbol{x}_i, t)$, and observed seismograms $u_j^{obs}(\boldsymbol{x}_i, t)$, with an additional stabilizing constraint on the scalar seismic moment M_{0fix} fixed from the previous centroid analysis,

$$\Lambda = \frac{1}{2L_u} \int_0^T \sum_{i,j} \left[u_j(\boldsymbol{x}_i, t) - u_j^{obs}(\boldsymbol{x}_i, t) \right]^2 dt - \frac{1}{2M_{0fix}^2} \left[M_0 - M_{0fix} \right]^2 \tag{2}$$

where the summations are over stations (i) and components (j), M_0 represents scalar seismic moment corresponding to $s(\xi, t)$ and L_u is the L2 norm of the observed data.

The best fitting model can be found by minimization of the misfit, which can be approached in many ways. Due to the large number of model parameters (in principle an infinite number because the slip is a continuous function of fault position and time), we adopt a technique analogous to time-reverse methods used typically in the adjoint seismic tomography studies (Tromp et al., 2005, Fichtner et al., 2006). In such methods, gradient of the misfit with respect to the model parameters is analytically derived and then used in minimization procedure based on, e.g., conjugate gradient techniques.

Realizing that the misfit (2) is a function of model parameters $s(\xi, t)$ via functionals $u_j(\boldsymbol{x}_i, t)$ and M_0, we can write the Fréchet differential of Λ (i.e. infinitesimal change of misfit due to infinitesimal changes of the slip model, $Ds(\xi, t)$),

$$D\Lambda = \frac{1}{L_u} \int_0^T \sum_{i,j} \left[u_j(\boldsymbol{x}_i, t) - u_j^{obs}(\boldsymbol{x}_i, t) \right] Du_j(\boldsymbol{x}_i, t) dt - \frac{1}{M_{0fix}^2} \left[M_0 - M_{0fix} \right] DM_0 \tag{3}$$

$$Du_j(\boldsymbol{x}_i, t) = \int_0^T \int_0^L H(\boldsymbol{x}_i; \xi, t-\tau) Ds(\xi, \tau) d\xi d\tau \tag{4}$$

$$DM_0 = \int_0^T \int_0^L \mu W Ds(\xi, \tau) d\xi d\tau \tag{5}$$

Symbol μ represents the rigidity. Inserting (4) and (5) into (3) and realizing that the integration over t represents a convolution with time-reversed impulse response H, yields

$$\begin{aligned} D\Lambda &= \int_0^T \int_0^L \left(\frac{1}{L_u} \sum_{i,j} H(\boldsymbol{x}_i; \xi, -\tau) \star \left[u_j(\boldsymbol{x}_i, \tau) - u_j^{obs}(\boldsymbol{x}_i, \tau) \right] - \right. \\ & \left. \frac{1}{M_{0fix}^2} \left[M_0 - M_{0fix} \right] \mu W \right) Ds(\xi, \tau) d\xi d\tau. \end{aligned} \tag{6}$$

In equations (6) we can rename τ to t, obtaining equation (2) from the main article,

$$\begin{aligned} D\Lambda &= \int_0^T \int_0^L \left(\frac{1}{L_u} \sum_{i,j} H(\boldsymbol{x}_i; \xi, -t) \star \left[u_j(\boldsymbol{x}_i, t) - u_j^{obs}(\boldsymbol{x}_i, t) \right] - \right. \\ & \left. \frac{1}{M_{0fix}^2} \left[M_0 - M_{0fix} \right] \mu W \right) Ds(\xi, t) d\xi dt. \end{aligned} \tag{7}$$

Assuming the slip function is non-negative, we substitute $Ds(\xi, t) = s(\xi, t) D \ln s(\xi, t)$, where $D \ln s$ represents relative changes of the slip function. Equation (7) is then modified to

$$\begin{aligned} D\Lambda &= \int_0^T \int_0^L \left(\frac{1}{L_u} \sum_{i,j} H(\boldsymbol{x}_i; \xi, -t) \star \left[u_j(\boldsymbol{x}_i, t) - u_j^{obs}(\boldsymbol{x}_i, t) \right] - \right. \\ & \left. \frac{1}{M_{0fix}^2} \left[M_0 - M_{0fix} \right] \mu W \right) s(\xi, t) D \ln s(\xi, t) d\xi dt \end{aligned} \tag{8}$$

Note that the latter step introduces an implicit positivity constraint on the slip function.

The above mentioned formulation has been derived for a line fault model. Let us emphasize that generalization to a 2D fault model is straightforward. The line fault approximation was assumed in our particular application to the Movri Mountain earthquake as tests on both real data and synthetics showed almost no sensitivity to the source depth.

Numerical implementation

For numerical reasons $s(\xi, t)$ has to be expressed using some basis functions. Perhaps the simplest choice is to consider piece-wise constant functions with steps $\Delta\xi$ and Δt in space and time, respectively. This leads to discretization of the integrals in equation (8),

$$\begin{aligned} D\Lambda &= \sum_{k,l} K_{kl} D \ln s(\xi_k, t_l) \\ K_{kl} &= \left(\frac{1}{L_u} \sum_{i,j} H(\boldsymbol{x}_i; \xi_k, -t_l) \star \left[u_j(\boldsymbol{x}_i, t_l) - u_j^{obs}(\boldsymbol{x}_i, t_l) \right] - \right. \\ & \left. \frac{1}{M_{0fix}^2} \left[M_0 - M_{0fix} \right] \mu W \right) s(\xi_k, t_l) \Delta\xi \Delta t \end{aligned} \tag{9}$$

where summation over k and l is over spatial and time samples, respectively; $s(\xi_k, t_l)$ are the amplitudes of the discretized slip function and K_{kl} represents the corresponding gradient of the misfit function in the model parameter. With K_{kl} at hand one can utilize, e.g., the conjugate gradient method (Press et al, 1992) to minimize misfit (2) with the implicit positivity constraint.

Synthetic test

To test our slip inversion approach, we created a synthetic forward source model (see Figure A1a) that resembles the results obtained for the Movri Mountain earthquake. The delayed asperity is incorporated. The synthetic seismograms have been then inverted (assuming the same stations and frequency range).

The individual iterations are presented in Figure A1b. The inversion performs similarly as in the real case, see Figure 2a in the main text. The first iterations reveal the main direction of the rupture propagation. Starting with the 6th iteration the slip patch in the middle of the fault splits. The other iterations only slightly change the resulting model, which corresponds to only minor changes in the variance reduction. The slip models correctly reveal the three major slip segments, including the delayed asperity. The only less well reproduced feature is the partial rupture propagation to the south-west (left part of the figures). Furthermore, Figure A1c shows comparison between the input and the inverted source models in terms of the moment rate (left) and the distribution of moment release on the fault (right). The fit is relatively good, correctly tracing the main episodes in time and spatial domains.

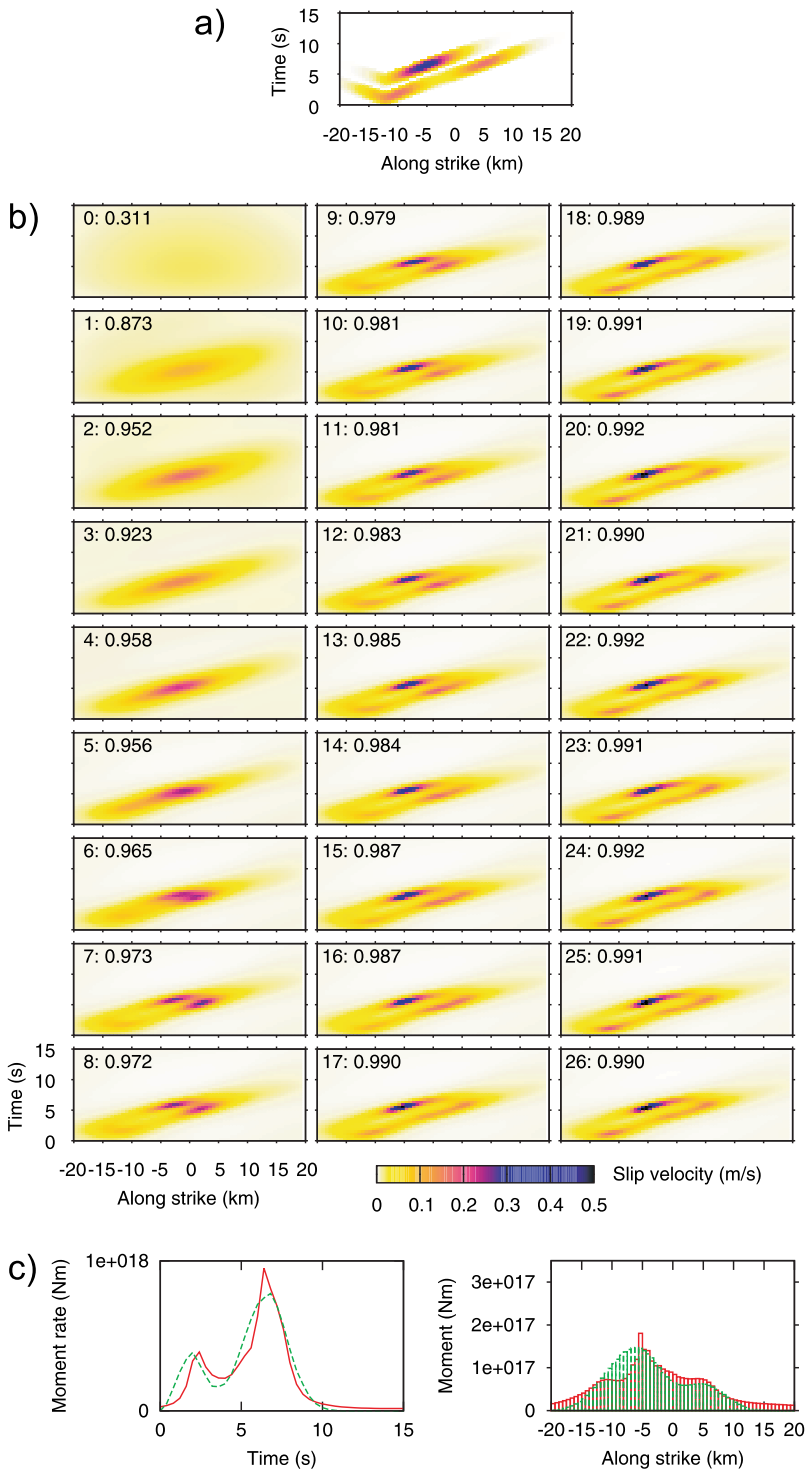

Figure A1. Synthetic test of the inversion method. a) Input source model to be inverted. b) Iterations of the slip inversion. The inscribed numbers represent the number of iteration and the corresponding variance reduction. c) Comparison between the input (green) and the inverted (red) rupture models in terms of the moment rate (left) and the distribution of moment release on the fault (right).

Additional figures

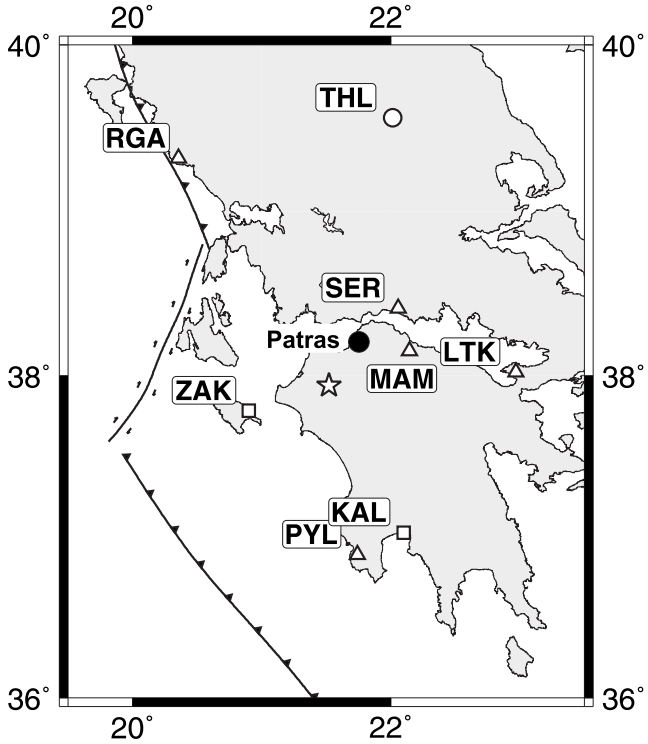

Figure A2. Distribution of stations used in the present study. Symbols refer to the station network: ITSAK (squares), NOA (circle), PSLNET (triangles). Main tectonic lines of the western Greece are displayed.

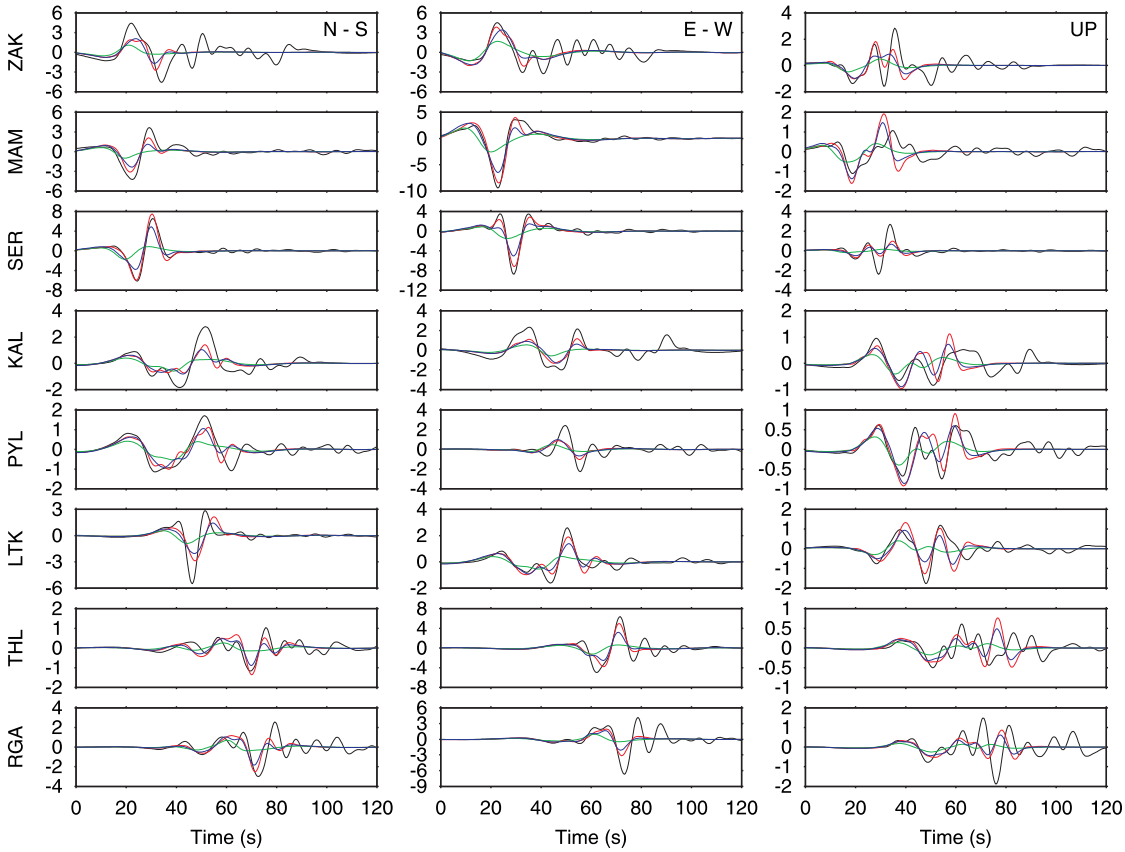

Figure A3. Matching data with synthetics. Near regional waveforms up to 0.2 Hz (displacement in millimeters), plotted in black, are compared with synthetic seismograms for three iterations, 0 (green), 1 (blue) and 26 (red). The station codes appear at left, see also Figure A2.

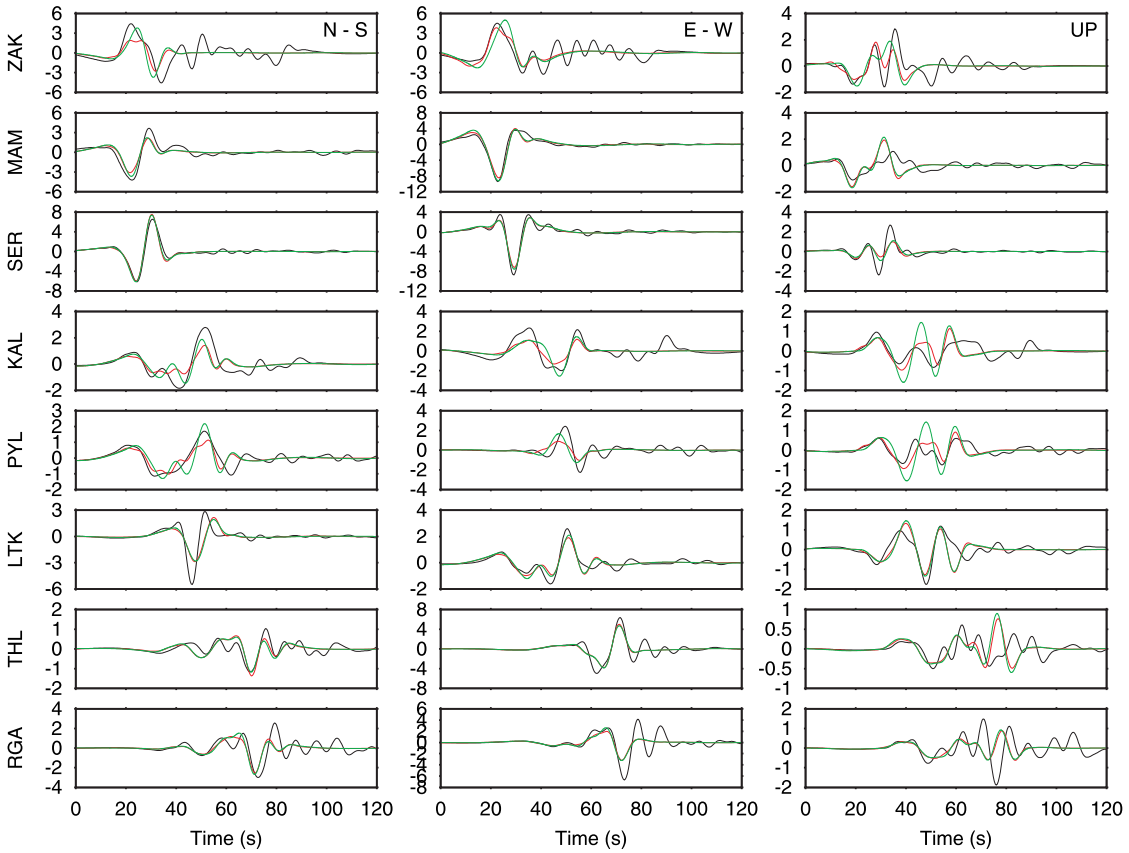

Figure A4. Same as Figure A3, only the observed waveforms (black) are compared with synthetic seismograms for the CMT solution (green) and the 26th iteration of the slip inversion (red). Note especially the better fit of the duration of dominant pulses for the distributed slip model.